

Boroxol rings and the stochastic matrix method

G.G. Naumis and R.A. Barrio

Instituto de Física, Universidad Nacional Autónoma de México, Apartado postal 20-364, 01000 México, D.F., Mexico

R. Kerner and M. Micoulaut

Laboratoire GCR, Tour 22-12, 4-eme étage, Boîte 142 Université Pierre et Marie Curie, 4. Place Jussieu, 75005 Paris, France

Recibido el 10 de enero 1998; aceptado el 6 de marzo 1998

A statistical model based on the stochastic matrix method is developed and used to find the fraction of boron atoms belonging to boroxol rings in a boron oxide (B_2O_3) glass. These results are compared with recent experimental data from inelastic neutron scattering estimates. The method also allows to evaluate the energies related to the formation of a single B-O-B unit in an oxygen bridge or in a boroxol ring. The qualitative behavior of the heat capacity $C_p(T)$ during the glass transition is reproduced, with the inflexion point at the temperature given by the experiment. The model gives a reasonable qualitative prediction for the growth of micro-clusters.

Keywords: Glass transition; glasses; boron oxide

Se desarrolla un modelo estadístico basado en el método de la matriz estocástica y se usa para encontrar la fracción de átomos de boro pertenecientes a anillos boroxol en un vidrio de óxido de boro (B_2O_3). Estos resultados se comparan con datos experimentales recientes de estimaciones de dispersión inelástica de neutrones. El método permite también evaluar las energías relacionadas a la formación una unidad simple B-O-B en un puente de oxígeno o en un anillo boroxol. El comportamiento cualitativo del calor específico $C_p(T)$ durante la transición vítrea se reproduce, con el punto de inflexión a la temperatura dada por el experimento. El modelo da una predicción cualitativa razonable para el crecimiento de micro-cúmulos.

Descriptores: Transición vítrea; vidrios; óxido de boro

PACS: 64.70.Pf; 61.43.Fs; 61.43.Bn

1. Introduction

Boroxol rings are particular structures that have been suggested to exist in great numbers in vitreous B_2O_3 . They represent the best example of intermediate range order, as defined by Galeener [1] and are six-membered planar and regular rings B_3-O_3 in which there should be a substantial reduction of the oxygen-bridge angle, since the average O-B-O angle in the network is 130° . The abundance of boroxol rings in the network should be substantial to explain the experiments, particularly the extremely sharp peaks found in vibrational spectroscopic studies, as Infrared and Raman scattering [2, 3]. However, the existence of boroxol rings in the correct concentrations has been questioned, due to the fact that recent molecular dynamics calculations have found it difficult to produce boroxol rings, claiming that they are not needed to explain most of the experimental data. One should mention that there is not yet a model of a structure containing many boroxol rings able to predict the density of the material.

There are various kinds of theoretical calculations, ranging from effective medium models [4]; to more detailed ones [5], which are able to explain all the experimental features only if one assumes large quantities of boroxol rings in the disorder network. A more definite argument in favour of the existence of boroxol rings comes from recent neutron scattering experiments [6], which can be explained coherently only if $\sim 80\%$ of the Boron atoms belong to rings.

This paper has the purpose of settling this question about the existence and abundance of boroxol rings in the amorphous network of boron oxide. Evidently, the formation of rings should be a consequence of the way the solid is grown, since they are not present in any of the crystalline forms of B_2O_3 , and some kinetic models are needed to explain their formation. Molecular dynamics is unlikely to give definite answers, since the main reason for the formation of rings should be a peculiar three body force that allows to modify the bridge angle. Therefore, we have developed a theoretical model for the solid growth, based on the original ideas given in Refs. 7-10, and applying the stochastic matrix method for solid growth, first put forward by Kerner [11]. The complete and detailed description of the method can be found in a former paper [12].

2. Stochastic matrix method description of the growth of a solid

Let us start by assuming that while cooling down the melt, some clusters of atoms are formed through an agglomeration process. During the solid growth through agglomeration, many complicated and competing processes take place, but gradually, bigger clusters and parts of the network appear everywhere. Whatever their shape, they can be divided in two parts: the *rim*, (or the *border*), composed of all the entities that offer a potential possibility for a new entity to stick and

TABLE I. Calculated values of the isotopic coefficient (α) for the first few excited states, for the ϕ^4 double-well and the quadratic double-well symmetric (QDW-s) and asymmetric (QDW-a) potentials.

State (n)	ϕ^4	QDW-s	QDW-a
1	0.7436	0.8797	0.8832
2	0.7083	0.6573	0.7036
3	0.7288	0.6495	0.6524
4	0.6925	0.6246	0.6225
5	0.6964	0.6190	0.6099
6	0.6873	0.6093	0.6050
7	0.6876	0.5979	0.5979

amplitudes, and the quartic potential for the ϕ^4 double-well potential. From a dimensional analysis of the Schrödinger equation it is easy to show that the isotopic coefficient of the quartic potential is $\alpha = 2/3$. The asymmetry of 6% in the QDW potential produces a small change in the isotopic coefficient values (see figure 2), however this change is not the same for all excited states. The largest change found was for the second excited state $\sim 7\%$ with respect to the symmetric case, therefore the asymmetry in the potential has not an important effect on the isotopic coefficient.

In Table II we present the calculated value of the isotope frequency shift ($\Delta\omega/\omega$) for the states 2 and 3 when the isotopic mass of oxygen is changed from O^{16} to O^{18} , these modes correspond to the Raman and infrared active modes observed experimentally at $\sim 500 \text{ cm}^{-1}$ and $\sim 570 \text{ cm}^{-1}$ respectively. The experimental value of the isotope frequency shift and the result from the shell model (harmonic) for these two modes are also presented [6–8]. We can see that the calculations of the isotope shifts using rigid double-well potentials differ from the experimental values even more than those found using the shell model (harmonic potentials). Therefore, both anharmonic potentials ϕ^4 and QDW are unable to reproduce

TABLE II. Optical shift frequencies in $YBa_2Cu_3O_7$. Experimental and calculated values of $\Delta\omega/\omega(\%)$ for the Raman ($n = 2$) and Infrared ($n = 3$) modes.

Mode	Exp.	Shell model	ϕ^4	QDW-s	QDW-a
Raman ($n = 2$)	4.70 ^a	5.60 ^a	6.37	5.96	5.95
Infrared ($n = 3$)	3.60 ^b	4.33 ^c	6.30	5.93	5.92

^a Ref. 7. ^b Ref. 6. ^c Ref. 8.

the experimental values of the isotopic coefficient (frequency shift) despite that these potentials reproduce the local structure observed with EXAFS [1]. This result suggests the presence of a different kind of anharmonicity in the dynamic of the axial oxygen, possibly polaronic behavior [12].

4. Summary

We have calculated the isotopic coefficient for the first few excited states of two anharmonic potential, the ϕ^4 double-well potential and the QDW potential, when the isotopic mass of oxygen is varied from 14–20 uma. For all excited states the isotopic coefficient differs from the harmonic value as is expected in anharmonic potentials, however it approaches the limiting value of $2/3$ in the case of the ϕ^4 potential and to the value of $1/2$ in the case of the QDW potential for high energy states. Both anharmonic potentials ϕ^4 and QDW are unable to reproduce the experimental values of the isotopic coefficient (frequency shift), suggesting the presence of a different kind of anharmonicity like polaronic behavior.

Acknowledgments

This work was supported by the Consejo Nacional de Ciencia y Tecnología (CONACyT, México) under Grants No. 3868P-E9608 and No. 3967P-E9608.

*. Departamento de Física, Centro de Investigación y de Estudios Avanzados del Instituto Politécnico Nacional, México D.F., Mexico.

- J. Mustre de León, S.D. Conradson, I. Batistic, and A.R. Bishop, *Phys. Rev. Lett.* **65** (1990) 1675; J. Mustre de León *et al.*, *Phys. Rev. B* **45** (1992) 2447.
- P.G. Allen, J. Mustre de León, S.D. Conradson, and A.R. Bishop, *Phys. Rev. B* **44** (1991) 9480.
- D. Haskel *et al.*, *Phys. Rev. B* **56** (1997) R521.
- B.H. Toby, T. Egami, J.D. Jorgensen, and M.A. Subramanian, *Phys. Rev. Lett.* **64** (1990) 2414.
- T. Egami *et al.*, *Physica C* **185–189** (1991) 867.
- M.K. Crawford, W.E. Farneth, E.M. McCarron III, and R.K. Bordia, *Phys. Rev. B* **38** (1988) 11382.
- G. Ruani *et al.*, *Physica C* **226** (1994) 101; D. Palles *et al.*, *Phys. Rev. B* **54** (1996) 6721.
- R. Heen, T. Strach, E. Schönherr, and M. Cardona, *Phys. Rev. B* **55** (1997) 3285.
- A.R. Bishop *et al.*, *Z. Phys. B. Cond. Matt.* **76** (1989) 17; T. Galbaatar *et al.*, *Physica C* **176** (1991) 496; V.H. Crespi and M.L. Cohen, *Phys. Rev. B* **48** (1993) 398.
- J. Mustre de León *et al.*, *Phys. Rev. Lett.* **68** (1992) 3236.
- M.I. Salkola, A.R. Bishop, J. Mustre de León, and S.A. Trugman, *Phys. Rev. B* **49** (1994) 3671; M.I. Salkola, A.R. Bishop, S.A. Trugman, and J. Mustre de León, *Phys. Rev. B* **51** (1995) 8878.
- J. Mustre de León *et al.*, *Rev. Mex. Fís.* **44 S3** (1998) 122.

agglomerate, and the *bulk*, (or the *interior*), that is, all the units that have satisfied all their bonds already.

The elementary entities composing the rim are found in a finite (usually quite small) number of local geometrical situations offering one, two or more possibilities for another entity to stick to. We shall call them *sites*, and we shall assume that the probability of a simultaneous agglomeration of two or more atoms at a single site is negligible.

While the temperature slowly decreases, the average size of clusters grows due to the progressive agglomeration of new atoms that stick to the rim. After a characteristic time a new layer of atoms is created, thus transforming the probabilities of observing various sites on the rim.

This process of growth at the rim can be described by a linear transformation, represented by a matrix acting on a vector, whose components are the probabilities of finding a given site on the rim of a cluster. The matrix transforms this vector into a new one, because the rim is changed after adding one atom to the cluster. The transformation of the rim depends on the site on which the new atom sticks. Now, each sticking process has a certain probability to occur, thus, the matrix elements contain the probabilities of transforming each kind of site into others. The probability factors should include two contributions: (1) the statistical weight for each process, that is, the number of ways leading to the same final result, and (2) the Boltzmann factor taking into account the energy barrier of forming a certain kind of bond.

Let us apply these ideas to the B_2O_3 continuous network. The elementary unit, dictated by the bond chemistry is a triangle $B(O_{\frac{1}{2}})_3$ [9]), which we shall call a "singlet". Two singlets can be connected only using one bond to form a "doublet", since other ways of connecting two units would produce a two-fold ring which is not seen in the real network. Let us assume that the energy cost to form this bonding is E_1 . After a doublet is produced, two situations can occur if a new singlet is added: the newly arriving singlet forms a longer chain (a "triplet") or it can close a ring, with a different energetic cost (E_2), since one has to deform the bridge angles in a ring. The agglomeration process occurs at a given temperature T , at which the individual bonds reach equilibrium. Therefore, we shall use the notation:

$$e^{-\epsilon} = e^{E_1/kT},$$

and

$$e^{-\eta} = e^{E_2/kT}.$$

where k is the Boltzmann constant.

The possible configurations, or sites are shown in Fig. 1. We shall denote these configurations by x, y, z, t, u, w . In principle one could have also considered longer chains of singlets, but this would lead to the multiplication of sites and transitions not expected in a real glass, since the creation of longer chains in covalent glasses is negligible, because one should avoid the formation of local voids.

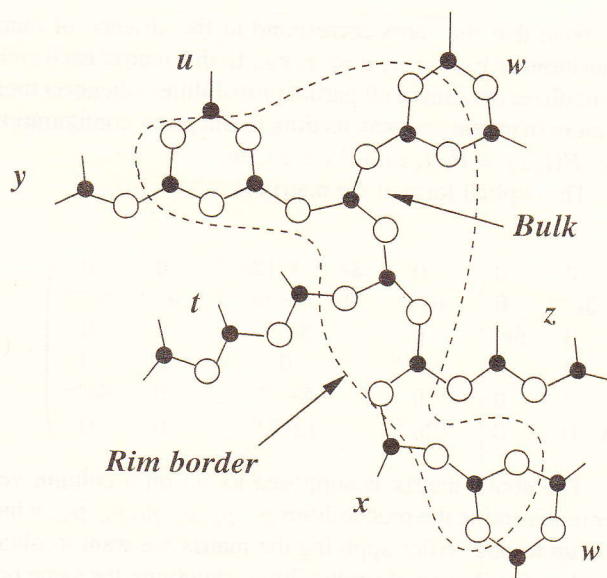


FIGURE 1. A typical cluster in vitreous B_2O_3 showing the six types of sites considered on the rim.

The transition probability for each elementary step can be given in the following way;

$$x \Rightarrow y : P(x, y) \sim 3e^{-\epsilon},$$

$$y \Rightarrow z : P(y, z) \sim 6e^{-\epsilon},$$

$$z \Rightarrow \begin{cases} y & : P(z, y) \sim 2 \times 3e^{-\epsilon}, \\ \text{or } t & : P(z, t) \sim 6e^{-\epsilon}, \\ \text{or } w & : P(z, w) \sim 12e^{-\eta}, \end{cases}$$

$$t \Rightarrow \begin{cases} y + z & : P_1(t, y) \text{ and } P(t, z) \sim 3e^{-\epsilon}, \\ \text{or } x + 2y & : P_1(t, x) \text{ and } P_2(t, y) \sim 3e^{-\epsilon}, \\ \text{or } y + u & : P_3(t, y) \text{ and } P(t, u) \sim 12e^{-\eta}, \\ \text{or } x + w & : P_2(t, x) \text{ and } P(t, w) \sim 12e^{-\eta}, \end{cases}$$

$$u \Rightarrow x : P(u, x) \sim 3e^{-\epsilon},$$

$$w \Rightarrow y + u : P(w, y) \text{ and } P(w, u) \sim 6e^{-\epsilon}.$$

Here we took into account the purely statistical factors according to the number of free bonds and the multiplicity available for each transition, which can be quite easily found out from purely geometrical considerations, and the Boltzmann factors according to the new bonds formed.

The factors $P(x, x), P(x, y), \dots$ etc., that define statistical weights of transitions resulting in the corresponding transformations of sites can be displayed as a 6×6 matrix:

$$\begin{pmatrix} 0 & 0 & 0 & P(t, x) & 0 & 0 \\ P(x, y) & 0 & P(z, y) & P(t, y) & P(u, y) & P(w, y) \\ 0 & P(y, z) & 0 & P(t, z) & 0 & 0 \\ 0 & 0 & P(z, t) & 0 & 0 & 0 \\ 0 & 0 & 0 & P(t, u) & 0 & P(w, u) \\ 0 & 0 & P(z, w) & P(t, w) & 0 & 0 \end{pmatrix}.$$

Note that the zeros correspond to the absence of many transitions, e.g. $x \Rightarrow x$, $y \Rightarrow x$, etc. In this matrix each entry symbolizes the sum of all partial probabilities whenever there is more than one pathway leading to the given configuration, e.g. $P(t, x) = P_1(t, x) + P_2(t, x)$, etc.

The explicit form of the matrix is

$$\begin{pmatrix} 0 & 0 & 0 & 3e^{-\epsilon} + 12e^{-\eta} & 0 & 0 \\ 3e^{-\epsilon} & 0 & 6e^{-\epsilon} & 9e^{-\epsilon} + 6e^{-\eta} & 3e^{-\epsilon} & 6e^{-\epsilon} \\ 0 & 6e^{-\epsilon} & 0 & 3e^{-\epsilon} & 0 & 0 \\ 0 & 0 & 6e^{-\epsilon} & 0 & 0 & 0 \\ 0 & 0 & 0 & 6e^{-\eta} & 0 & 6e^{-\epsilon} \\ 0 & 0 & 12e^{-\eta} & 12e^{-\eta} & 0 & 0 \end{pmatrix}. \quad (1)$$

The above matrix is supposed to act on a column vector representing the probabilities $p_x, p_y, p_z, p_t, p_u, p_w$, which add up to one. After applying the matrix we want to obtain another distribution of probabilities, satisfying the same normalization condition. Therefore the sum of the entries in each column of the above matrix must be set to one. After normalization, we get a stochastic matrix (M) that transforms the probabilities of finding one configuration on the rim of a cluster, $(p_x, p_y, p_z, p_t, p_u, p_w)$ into a new set of probabilities $(p'_x, p'_y, p'_z, p'_t, p'_u, p'_w)$ after an entire new layer of atoms has been grown, with one new atom at each available site:

$$M = \begin{pmatrix} 0 & 0 & 0 & \frac{1+4\xi}{5+12\xi} & 0 & 0 \\ 1 & 0 & \frac{1}{2+2\xi} & \frac{5+12\xi}{5+12\xi} & 1 & \frac{1}{2} \\ 0 & 1 & 0 & \frac{1}{5+12\xi} & 0 & 0 \\ 0 & 0 & \frac{1}{2+2\xi} & 0 & 0 & 0 \\ 0 & 0 & 0 & \frac{2\xi}{5+12\xi} & 0 & \frac{1}{2} \\ 0 & 0 & \frac{2\xi}{2+2\xi} & \frac{4\xi}{5+12\xi} & 0 & 0 \end{pmatrix}.$$

Using the above matrix, the growth of clusters is modelled by a successive application of the matrix on an arbitrary initial vector \mathbf{v}_0 . Thus, the evolution of the probabilities on the rim after j steps is given by

$$\mathbf{v}_j = M^j \mathbf{v}_0. \quad (2)$$

The final configuration depends only on the eigenvectors of the stochastic matrix. It is easy to prove that a matrix with all the columns normalized to one has at least one eigenvalue equal to one, while the others can be real, complex or imaginary, depending on the values of the parameters involved. The complex eigenvalues indicate the presence of an *oscillatory regime* of growth, usually damped by the norm of the eigenvalue, if it is less than 1. Due to this exponential damping, only eigenvectors with norm one remain after **many** successive applications of the stochastic matrix. If we suppose that M has only one such eigenvalue ($\lambda_1 = 1$), with eigenvector

\mathbf{e}_1 , then, in the limit of large j , \mathbf{v}_j converges to this eigenvector, independently of the initial conditions.

As a consequence, the evolution of the rim attains a stable statistical regime after successive steps of growth; this regime is governed solely by the statistics represented by the eigenvector with eigenvalue one. This eigenvector determines the distribution $(p_x, p_y, p_z, p_t, p_u, p_w)_\infty$ to which the averaged statistics tends asymptotically. This is also the statistics of the bulk if the clusters are really large. For clusters of intermediate size, one should rather average over the sum of many layers.

3. The statistical analysis of boroxol rings

In our statistical model for the B_2O_3 glass, the only free parameter is ξ , or the excess free energy when closing a ring $(E_2 - E_1) = kT \ln(\xi) = \mathcal{F}$. To fix this parameter, we shall study the behavior of the internal energy U , and the specific heat c_p , near the glass transition temperature, and then fit the result with available experimental data.

The internal energy involved in a process of growing in the i -th layer is,

$$\frac{3kT}{2} - E_2 P_B^i(T) - E_1 [1 - P_B^i(T)],$$

where the first term is the kinetic contribution, and $P_B^i(T)$ is the probability of forming a ring from the i -th rim to the $i+1$, simply obtained by counting the proportion of rings that were formed during this process. This information is encoded in the matrix as the probability of the processes: $z_i \rightarrow w_{i+1}$ and $t_i \rightarrow u_{i+1}, w_{i+1}$. Then,

$$P_B^i(T) = p_{z_i} (M_{63}) + p_{t_i} (M_{54} + M_{64}).$$

Now, the internal energy is an extensive parameter, the total energy after N steps of growing is the sum of the energies in each layer of the growth:

$$U(T) = \frac{3NkT}{2} + E_1 N + (E_2 - E_1) \sum_{i=1}^N P_B^i(T).$$

The specific heat is obtained by taking the derivative of U with respect to the temperature,

$$c_p(T) = \frac{3Nk}{2} + (E_2 - E_1) \sum_{i=1}^N \frac{dP_B^i(T)}{dT}. \quad (3)$$

and if we calculate $c_p(T)$ for a big number of steps of growing, then $P_B^i(T)$ can be replaced by its limit value on the stationary regime,

$$c_p(T) = \frac{3Nk}{2} + (E_2 - E_1) N \frac{dP_B^\infty(T)}{dT}. \quad (4)$$

In glasses, it is generally observed that there is an inflection point and a precipitous decrease in the heat capacity [1] at the glass transition temperature (T_g). Therefore, we d

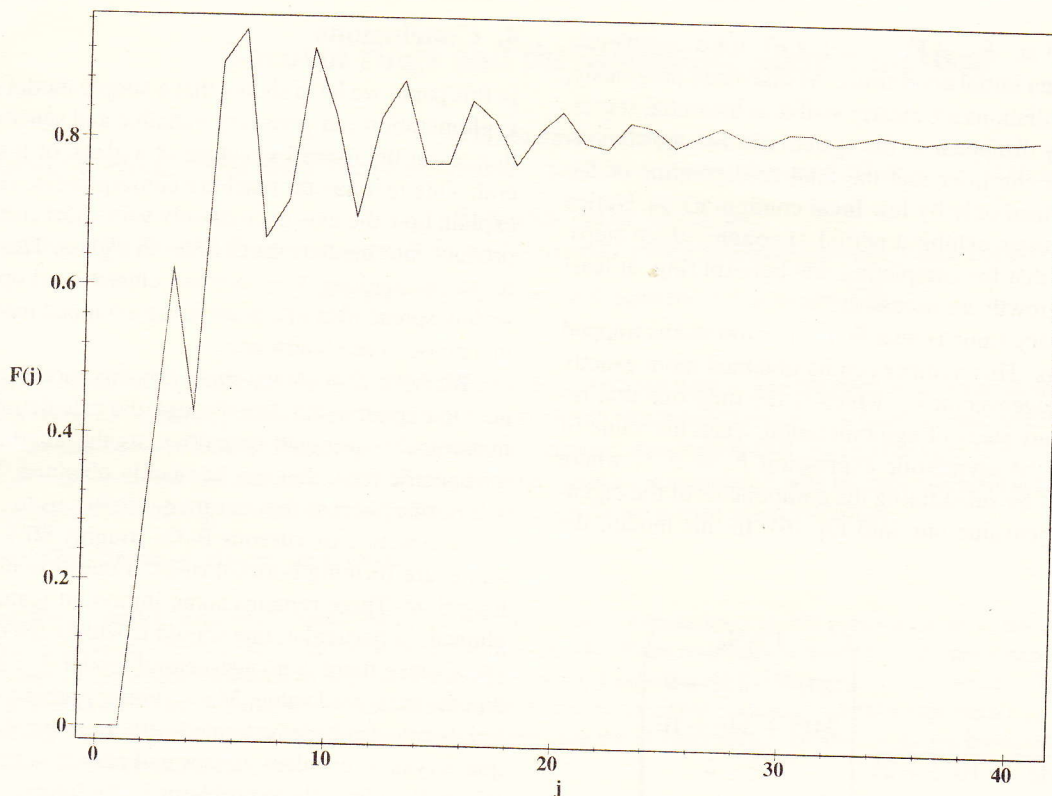


FIGURE 2. Example of the evolution of $F(j)$ as a function of the agglomeration step j .

mand that

$$\frac{\partial^2}{\partial^2 T} [c_p(T)]_{T=T_g} = 0,$$

and by using (4) we get,

$$\frac{d^3}{d^3 T} [P_B^\infty(T)]_{T=T_g} = 0. \quad (5)$$

The latter condition fixes the parameter ξ at T_g , and this quantity is well known from various experiments to vary from $T_g = 470$ K to 530 K (see Ref. 14). For $T_g = 470$ K, we have found that condition (5) is satisfied for two values:

- 1) $E_2 - E_1 = 0.214$ eV = 4.927 Kcal/mol,

and

- 2) $E_2 - E_1 = 0.068$ eV = 1.566 Kcal/mol.

However, only the first one corresponds to the real glass, since only this energy difference leads to the correct behavior of $c_p(T)$. Another fitting is possible when $T_g = 530$ K, which gives,

$$E_2 - E_1 = 0.242$$
 eV = 5.572 Kcal/mol.

These values are very close to other estimates found in the literature. Walrafen and co-workers [14] have found 6.4 ± 0.04 Kcal/mol, obtained from experimental data. Snyder [15] estimated 6.0 Kcal/mol, obtained from *ab initio* quantum mechanical calculations.

Once the energy difference ($E_2 - E_1$) is fixed, we can calculate the fraction of boron atoms in the glass that are in boroxol rings ($F = N_B/N_T$). At this point, we must remember that, in principle, the evolution of the vector v_j gives only information on the evolution of the probabilities on the rim, while the fraction F is a property of the bulk. However, this bulk is formed by the addition of consecutive layers. Therefore, by adding the number of atoms that are trapped into boroxol rings in each step of growing we can find N_B . Another problem remains to be solved: The creation of a ring needs three steps of agglomeration, thus, to be able to decide if an atom is inside a boroxol ring, we must consider more than one step of agglomeration.

This counting can be achieved in the following way: The number of boron atoms in boroxol rings expected in the j -th step is

$$N_B^j = u_j + w_j + 2z_j (M_{63}) + 2t_j (M_{54} + M_{64}),$$

and the fraction F is obtained by dividing this number by the total number of atoms on the rim, that is

$$F(j) = \frac{N_B^j}{x_j + y_j + 2z_j + 3t_j + u_j + 2w_j}. \quad (6)$$

In Fig. 2 we show the evolution of F as a function of the number of elementary steps of growth (j), with the energy

difference fixed at: $E_2 - E_1 = 0.214$ eV for a completely arbitrarily chosen initial conditions. As discussed previously, the damped oscillations are clearly visible at the initial stages, but they rapidly disappear as the system reaches the stationary regime. We can infer that the final configuration of the glass is determined only by few **local** configurations. Notice that the oscillations exhibit a period of roughly three steps, due to the fact that for completing one boroxol ring, at least three steps of growth are necessary.

The stationary value is near 80% of boron atoms trapped in boroxol rings. This number can be obtained more exactly if we use the eigenvector \mathbf{e}_1 , which is the only one that remains after many steps of agglomeration. Then the value of F is given by the asymptotic expression $F = F^\infty$, where F^∞ is obtained by substituting the components of the eigenvector with eigenvalue one into Eq. (6). In this model, the eigenvector is,

$$\mathbf{e}_1 = \frac{1}{84\xi^2 + 107\xi + 25} \begin{pmatrix} 1 + 4\xi \\ 24\xi^2 + 34\xi + 9 \\ 24\xi^2 + 34\xi + 10 \\ 12\xi + 5 \\ 3\xi(4\xi + 3) \\ 2\xi(12\xi + 7) \end{pmatrix}$$

Inserting the appropriate energy values for $T_g = 470$ K into the last expression we get that $F^\infty = 81.3\%$.

This result is in very good agreement with other theoretical and experimental results like the 83% proposed by Jellison *et al.* [16], 80% by Hannon *et al.* [17] and 84% by Micoulaut *et al.* [9].

4. Conclusions

In this paper we have shown that a simple model of statistical agglomeration can give very valuable and sensitive information about the overall structure of a glass, or a solid in general. This fact has far reaching consequences, since one can explain how the existence of only very short correlations can produce intermediate range order in a glass. This gives validity to calculations done in small clusters and opposes to the widely spread idea of a glass being a trapped metastable state in a phase-space landscape.

We have also shown that with this model one can connect to experimental data through the calculation of thermodynamically averaged quantities, as the internal energy, or the specific heat, that can be readily obtained. The main result of this paper is that our model forces us to conclude that in the structure of vitreous B_2O_3 roughly 80% of the boron atoms are forming boroxol rings, a question unsolved for a long time. There remains some important features to be explained, in particular, one should calculate the density of the glass, since there is no a structural model that is able to predict the measured value. Many similar problems in other materials can also be investigated with this simple technique, as quasicrystals, covalent glasses and nanostructured materials. We shall address these problems in the future.

Acknowledgments

This work was supported by the project IN104296 from UNAM-DGAPA, and by CONACyT grants 0088P-E, 2677P-E and 25237-E. GGN is grateful for the hospitality received at the Université Pierre et Marie Curie during a post-doctoral stay there.

1. F.L. Galeener, *J. Non-Cryst. Solids* **123** (1990) 182.
2. F.L. Galeener, G. Lucovsky, and J.C. Mikkelsen Jr., *Phys. Rev. B* **22** (1980) 3983.
3. M. Massot and M. Balkanski, in *MicroIonics, Solid State Integrable Batteries*, edited by M. Balkanski, (North Holland 1991) p.139.
4. R.A. Barrio, F.L. Castillo-Alvarado, and F.L. Galeener, *Phys. Rev. B* **44** (1991) 7313.
5. N. Uchida, T. Maekawa, and T. Tokokawa, *J. Non-Cryst. Solids* **74** (1985) 25.
6. A.C. Hannon, A.C. Wright, J.A. Blackman, and R.N. Sinclair, *J. Non-Cryst. Solids* **182** (1995) 78.
7. R. Kerner, *J. Non-Cryst. Solids* **135** (1991) 155; R. Kerner and M. Micoulaut, *J. Non-Cryst. Solids* **176** (1994) 271; R. Kerner, *Physica B* **215** (1995) 267.
8. D.M. dos Santos-Loff, R. Kerner, and M. Micoulaut, *Europhys. Lett.* **28** (1994) 573.
9. M. Micoulaut, R. Kerner, and D.M. dos Santos-Loff, *Europhys. Lett.* **7** (1995) 8035.
10. M. Micoulaut and R. Kerner, *J. of Phys.: Condens. Matter* **9** (1997) 2551.
11. R. Kerner, "Stochastic matrix method for modelling growth and agglomeration processes", (in press).
12. R.A. Barrio, R. Kerner, M. Micoulaut, and G.G. Naumis, *J. Phys.: Condens. Matter* **9** (1997) 9219.
13. S.R. Elliot 1990, *Physics of Amorphous Materials* (New York: Longman, 1989) p. 36.
14. G.E. Walrafen, S.R. Samanta, and P.N. Krishnan, *J. Chem. Phys.* **72** (1980) 113.
15. L.C. Snyder, *Bull. Am. Ceram. Soc.* **57** (1978) 825.
16. G.E. Jellison, L.W. Panek, P.J. Bray, and G.B. Rouse, *J. Chem. Phys.* **66** (1977) 802.
17. A.C. Hannon, R.N. Sinclair, and A.C. Wright, *Physica A* **201** (1993) 375.